The photoisomerization of a peptidic derivative of azobenzene: A nonadiabatic dynamics simulation of a supramolecular system

ARTICLE *in* CHEMICAL PHYSICS · JUNE 2008

Impact Factor: 1.65 · DOI: 10.1016/j.chemphys.2008.01.030

3 AUTHORS, INCLUDING:

Giovanni Granucci
Università di Pisa
80 PUBLICATIONS **1,920** CITATIONS
SEE PROFILE

Maurizio Persico
Università di Pisa
153 PUBLICATIONS **6,248** CITATIONS
SEE PROFILE

Available online at www.sciencedirect.com
ScienceDirect
Chemical Physics 349 (2008) 325–333
Chemical Physics
www.elsevier.com/locate/chemphys

The photoisomerization of a peptidic derivative of azobenzene: A nonadiabatic dynamics simulation of a supramolecular system

Cosimo Ciminelli, Giovanni Granucci, Maurizio Persico *

Dipartimento di Chimica e Chimica Industriale, Università di Pisa, v. Risorgimento 35, I-56126 Pisa, Italy

Received 11 December 2007; accepted 4 January 2008
Available online 30 January 2008

Abstract

The aim of this work is to investigate the mechanism of photoisomerization of an azobenzenic chromophore in a supramolecular environment, where the primary photochemical act produces important changes in the whole system. We have chosen a derivative of azobenzene, with two cyclopeptides attached in the *para* positions, linked by hydrogen bonds when the chromophore is in the *cis* geometry. We have run computational simulations of the *cis* → *trans* photoisomerization of such derivative of azobenzene, by means of a surface hopping method. The potential energy surfaces and nonadiabatic couplings are computed "on the fly" with a hybrid QM/MM strategy, in which the quantum mechanical subsystem is treated semiempirically. The simulations show that the photoisomerization is fast (about 200 fs) and occurs with high quantum yields, as in free azobenzene. However, the two cyclopeptides are not promptly separated, and the breaking of the hydrogen bonds requires longer times (at least several picoseconds), with the intervention of the solvent molecules (water). As a consequence, the resulting *trans*-azobenzene is severely distorted, and we show how its approach to the equilibrium geometry could be monitored by time-resolved absorption spectroscopy.

Keywords: Azobenzene; Supramolecular photochemistry; Photoisomerization; Semiempirical calculations; Surface hopping

1. Introduction

Azobenzene, along with a few other chromophores, is widely used as the reversibly photoswitchable unit to construct photoresponsive supramolecular systems. In recent reviews [1–7] one can find a host of applications. Materials of different kinds can undergo reversible changes, since the photoisomerization affects their density, optical properties, phase transition parameters, solubilities, micelle equilibria, permeability, and viscosity. The irradiation can very effectively induce alignment in fluid phases and easily detectable modifications of polymer surfaces (thus enabling us to write and erase information). Enzymes, DNA sequences, chelating agents and surfactants can be activated/deactivated using light. Threading or de-threading can be triggered in rotaxanes and pseudorotaxanes, and folding or unfolding in peptides.

In all of these examples the azobenzene unit is part of a supramolecular structure and its isomerization causes important changes in the whole system. In most cases, a scheme based on four chemical species can describe such changes. The azobenzene moiety is either *cis* or *trans*, and we assume the rest of the supramolecular system also can exist in two forms, which we shall call A and B. Then, we may have in principle the four species: *cis*-A, *cis*-B, *trans*-A and *trans*-B (see Fig. 1). Usually, in the ground state, the interconversion of *cis*-A and *cis*-B, or *trans*-A and *trans*-B, is much easier than the *cis–trans* isomerization. Suppose *cis*-A to be thermodynamically more stable than *cis*-B, and *trans*-A less stable than *trans*-B, in some specific conditions (temperature, concentrations etc). Then:

$$\Delta G(c\text{-A} \rightarrow c\text{-B}) > 0 \tag{1}$$

* Corresponding author. Tel.: +39 50 2219243; fax: +39 50 2219260.
E-mail address: mau@dcci.unipi.it (M. Persico).

0301-0104/$ - see front matter © 2008 Elsevier B.V. All rights reserved.
doi:10.1016/j.chemphys.2008.01.030

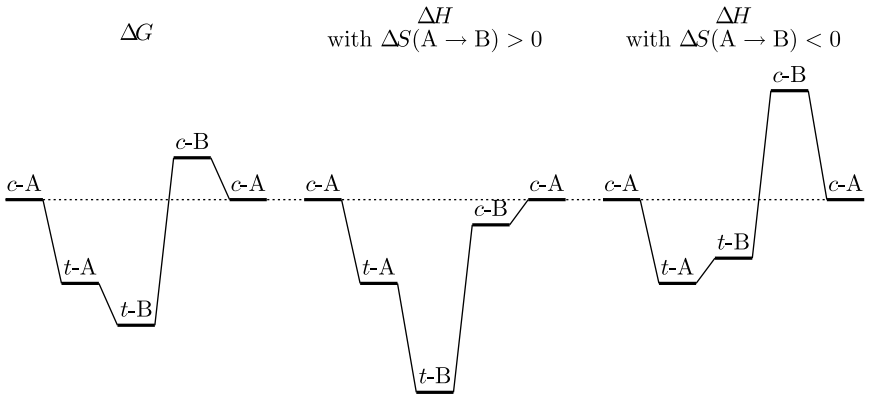

Fig. 1. First scheme: a hypothetic free energy profile for a supramolecular system with four possible structures, characterized by the *cis* or *trans* geometry of the photoisomerizable unit, and by two different states of its chemical environment. Second and third schemes: two enthalpy profiles, both consistent with the ΔG profile.

and

$$\Delta G(t\text{-A} \rightarrow t\text{-B}) < 0 \tag{2}$$

One of the interesting issues, concerning such systems, is the reaction time for the processes:

$$c\text{-A} \xrightarrow{h\nu} t\text{-A} \rightarrow t\text{-B} \tag{3}$$

and

$$t\text{-B} \xrightarrow{h\nu} c\text{-B} \rightarrow c\text{-A} \tag{4}$$

In fact, for applications such as the production of switches for computational purposes or data storage, the response times are crucial parameters. We can consider two limiting cases: (i) the *trans*-A and *cis*-B intermediates do not exist as stable species, and the photoreactions directly yield the final products; or, (ii) the second step of each sequence is just a ground state reaction, thermodynamically driven, with much longer reaction times than in case (i), depending on temperature. As an intermediate case, the second step can be a hot ground state reaction, in which the intermediate species rapidly converts into the final product, using part of the photon energy in the form of vibrational excitation.

Another important issue concerns the quantum yields of the photoreactions (3) and (4). They depend in the first place on the shape of the excited state potential energy surface (PES) of S_1, which is much less steep than the ground state one (see recent work by the theoretical photochemistry group of Bologna [8,9] and by our own [10,11]). A connection can be established between the slope of the excited state PES and the relative stabilities of the four chemical species. We first observe that important entropic changes can characterize the processes $t\text{-A} \rightarrow t\text{-B}$ and $c\text{-B} \rightarrow c\text{-A}$, for instance when they imply complexation, aggregation, or phase changes. On the contrary, we expect the isomerization reactions $t\text{-A} \rightarrow c\text{-A}$ and $t\text{-B} \rightarrow c\text{-B}$ to involve negligible entropy variations. Therefore, we can approximate all the relevant entropy changes as $\pm\Delta S(\text{A} \rightarrow \text{B})$. Eqs. (1) and (2) then become

$$\Delta H(t\text{-A} \rightarrow t\text{-B}) - T\Delta S(\text{A} \rightarrow \text{B}) < 0 \tag{5}$$

and

$$\Delta H(c\text{-B} \rightarrow c\text{-A}) + T\Delta S(\text{A} \rightarrow \text{B}) < 0 \tag{6}$$

They can be combined to yield

$$\Delta H(t\text{-A} \rightarrow t\text{-B}) + \Delta H(c\text{-B} \rightarrow c\text{-A}) < 0 \tag{7}$$

The schemes in Fig. 1 show two possible realizations of this inequality. Considering the thermodynamical cycle

$$c\text{-A} \rightarrow t\text{-A} \rightarrow t\text{-B} \rightarrow c\text{-B} \rightarrow c\text{-A} \tag{8}$$

we get

$$\Delta H(t\text{-B} \rightarrow c\text{-B}) + \Delta H(c\text{-A} \rightarrow t\text{-A}) > 0 \tag{9}$$

This means that at least one of the two photoreactions is more endothermic (or less exothermic), not just more endergonic, than in the case of the free azo chromophore, to which the equality $\Delta H(trans \rightarrow cis) + \Delta H(cis \rightarrow trans) = 0$ obviously applies. One or both photoreactions will be therefore hindered by the chemical environment of the chromophore. Since the electronic structure of the chromophore itself in most cases is not deeply affected, the excited state PESs are modified approximately in the same way as the ground state one, with respect to the free chromophore. If the ΔH of a photoreaction increases, the slope of the excited state PES becomes less favourable and the quantum yield of the reaction may decrease.

As an example that illustrates the above considerations, in this paper we describe the computational simulation of the *cis* → *trans* photoisomerization of a supramolecular azobenzene cyclopeptidic derivative (ABCP), which is strongly stabilized in the *cis* form. The system under study was synthesized and characterized by Reza Ghadiri and coworkers [12,13]. It consists of two essentially planar cyclooctapeptides (L-Cys-(D-Ala-L-Phe)$_3$-D-Ala), selectively methylated so that they can only form hydrogen bonds on one face of the ring. The two peptide rings are connected to the para positions of an azobenzene moiety by –CH_2–S–CH_2– bridges, the S atoms belonging to the cysteine residues (see Figs. 2 and 3). In the *cis* isomer of ABCP the peptide rings are coupled by up to eight intramolecular

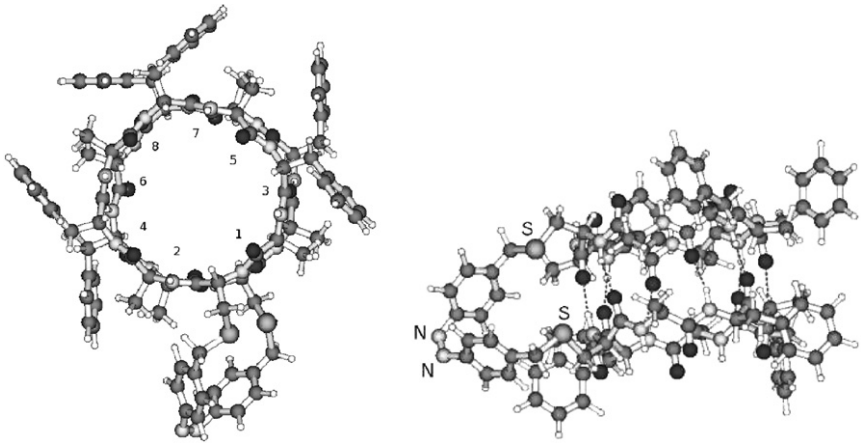

Fig. 2. Two views of the *cis* isomer of ABCP (in vacuo optimized geometry). In the left hand picture the aminoacid residues are numbered (same numbers for the two rings). In the right hand picture the S atoms and the azo N atoms are labelled.

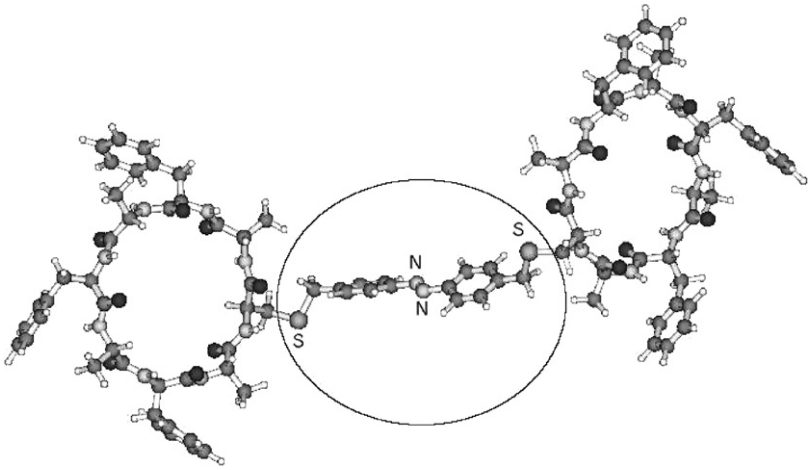

Fig. 3. The *trans* isomer of ABCP (in vacuo optimized geometry). The S atoms and the azo N atoms are labelled. An elliptic line encloses the QM atoms.

hydrogen bonds. In the *trans* isomer the two rings are held apart, and the hydrogen bonds are formed with other molecules, in the appropriate conditions. As a result, the two isomers exhibit quite different self-assembly properties, in solution as well as at the air–water interface and on solid supports. The system photoisomerizes in a perfectly reversible way, by using light of the appropriate wavelengths, although the quantum yields have not been determined.

Our aim is to investigate in detail the mechanism of the *cis* → *trans* photoisomerization of ABCP and to bring out the effect of the peptidic substituents and of their H-bond coupling on the reaction dynamics, on the excited state decay times, and on the quantum yields.

2. Method

We applied Tully's surface hopping representation of the nonadiabatic dynamics [14,15], with a direct calculation of the electronic energies and wavefunctions by a semiempirical QM/MM method [16–19]. We first optimized the geometry of ABCP derivative in vacuo, to characterize the *cis* and *trans* isomers and to compare with a previous computational study [20]. The only difference with the real molecule of Reza Ghadiri and co-workers [12,13] was that we dropped the protecting methyl groups that prevent the H-bonding on one face of the cyclopeptides, since this detail is not expected to play a role in the photodynamics. The simulations of the dynamics were run on ABCP with the addition of 103 water molecules, that influence the stability of the inter-peptidic H-bonds. The full system therefore contained 557 atoms, of which 30 were treated quantum mechanically in the electronic calculations (QM subsystem, highlighted in Fig. 3), and 527 were treated by a Molecular Mechanics force-field (MM subsystem).

We shall first outline the semiempirical QM/MM method [16–19] and give all the details that apply to the ABCP and ABCP + water systems. Next we shall describe the simulation procedure for the nonadiabatic dynamics. The structure of the semiempirical hamiltonian was the same as in the AM1 method, but the parameters were specifically reoptimized for the azobenzene molecule, to reproduce the available experimental data and ab initio results

[10]. We performed a truncated CI, with 259 determinants chosen within an active space of 10 electrons in 10 orbitals (MOs). The MOs were obtained by an SCF procedure with variable occupation numbers within the active space, which allows to represent correctly the breaking of the π bond by the CNNC dihedral angle of the azo group. The occupation numbers depend on the MO energies, and are self-consistently determined along with them [16,21]. Previous studies of the photodynamics of azobenzene itself [10,11] and of a cyclic derivative [19] were based on the same semiempirical hamiltonian and wavefunctions.

In the QM/MM treatment, the QM subsystem included the azobenzene moiety and the $–CH_2–S–$ groups attached in the 4 and 4′ positions (see Fig. 3). All other atoms made up the MM subsystem: the peptidic part of ABCP is treated by the FF98 force-field of AMBER7 [22] and the water molecules, when present, by the TIP3P model [23]. The QM/MM interaction hamiltonian contained three contributions [17]. The first is a Lennard-Jones term, representing the repulsion–dispersion forces between QM and MM atoms. The Lennard-Jones parameters were taken from AMBER7 also for the QM atoms. The second and third terms are the Coulomb interactions of the MM point charges with the core charges and the electrons of the QM atoms. The third term is added to the semiempirical hamiltonian and it influences the energies and wavefunctions of the QM subsystem in a state specific way. The boundary between the two subsystems was here represented by the S atoms, that were treated as "connection atoms" according to a proposal by Antes and Thiel [24]. The S atom parameters were the same as those determined for another azobenzene derivative in Ref. [18], except for the core charge. The latter depends on the atomic MM charges through an electroneutrality relationship [18], and in this case it was $q_S = 1.0602$.

The geometry optimization of ABCP in vacuo yielded the structures shown in Figs. 2 and 3, very similar to those obtained by Qu et al. [20] by the standard AM1 method. They found the *cis* isomer 1.35 eV more stable than the *trans* one. The total strength of the eight hydrogen bonds, computed by the B3LYP method with the 3-21G* basis set and BSSE correction, is about 0.33 eV larger than with AM1, so the $\Delta E_{cis–trans}$ would be about 1.7 eV at this computational level. We obtained $\Delta E_{cis–trans} = 2.25$ eV, largely as a result of the strong H-bonding interactions implemented in the FF98 force-field of AMBER7. In fact, such force-field was optimized for use with an explicit representation of the water solvent. It is clear that the $\Delta E_{cis–trans}$ values would greatly decrease by taking into account the interaction with water molecules, that form hydrogen bonds both with the carbonyl and with the amino groups of *trans*-ABCP. An accurate study of the relative stability of the two isomers in solution should include several thousands water molecules, even without taking into consideration the self-assembled structures.

To study the first stages of the *cis* → *trans* photoisomerization dynamics, we added to the *cis* isomer a minimum number of water molecules, initially located by using the "solvateCap" function of AMBER7, that creates a solvation sphere of a given radius, centered at the center of mass of the solute. With a radius of 13 Å, 103 water molecules were generated. In this way, all the hydrogen bonds were surrounded by a few water molecules. To obtain a Boltzmann distribution of nuclear coordinates and momenta, we ran a Brownian trajectory, with a temperature of 298 K, for 90 ps (see Refs. [10,16,25] for more details on the procedure and analogous applications). We discarded the first 10 ps, during which the kinetic and potential energies underwent large variations. During the next 80 ps, the kinetic energy oscillated around the average value of 22.2 eV, in agreement with the equipartition principle. We sampled the initial nuclear geometries and momenta for the excited state dynamics from this portion of the Brownian trajectory. A typical configuration is shown in Fig. 4.

The sampling of the initial conditions simulated an $n \rightarrow \pi^*$ excitation. The algorithm takes into account the probability of a vertical excitation, that is proportional to the squared transition dipole [25]. As a by-product of the sampling procedure, we obtained the absorption spectrum of the reactant. In our case, the simulated $n \rightarrow \pi^*$ band peaked at about 370 nm, with an HWHM of 70 nm. This is close to the result obtained for the free azobenzene molecule [10], and corresponds to a substantially unstrained state of the *cis* isomer. In fact, the initial conditions sampling yielded an average CNNC dihedral angle of $5.2 \pm 3.9°$, and NNC angles of $122.4 \pm 2.4°$, while the equilibrium values for isolated azobenzene are CNNC = 4.1° and NNC = 124.3°.

The surface hopping dynamics took into account four singlet states (from S_0 to S_3), as in our previous simulations for the isolated azobenzene molecule [10]. We applied Tul-

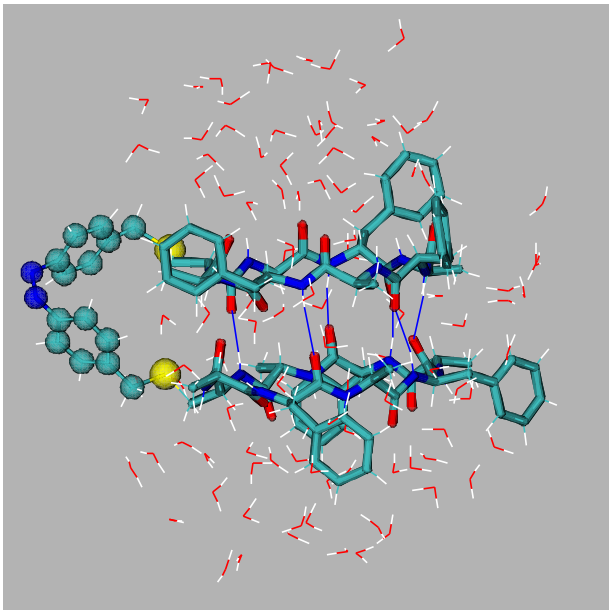

Fig. 4. A typical initial configuration for a trajectory describing the photoisomerization of ABCP.

ly's "fewest switches" algorithm [14,15], and we integrated the time-dependent Schrödinger equation (TDSE) with a method especially suited for PES crossing problems [16]. A Verlet third-order velocity formula was used to solve the Newton equations. The integration time step, both for the TDSE and for the nuclear trajectories, was 0.2 fs, and the trajectories were stopped 1500 fs after the vertical excitation. We ran a total of 171 trajectories. All calculations were run with a development version of the MOPAC package [26], where we have implemented our modifications of the semiempirical method, as well as the nonadiabatic dynamics.

3. Photoisomerization dynamics

Each trajectory was classified as "reactive" if the final CNNC angle, after 1500 fs, was in the range [140°, 180°], corresponding to a transoid geometry. All other trajectories turned out to have CNNC <20°, close to that of the *cis* isomer, and were classified as "unreactive". The computed quantum yield, i.e. the fraction of reactive trajectories, was 0.59. This value is practically identical to the quantum yield we computed for free azobenzene (0.61 [10]) and it falls within the range of experimental results for various solvents (0.40-0.69 [11]). It is clear that the photoisomerization is not hindered by the geometrical constraints due to the H-bonded peptide substituents.

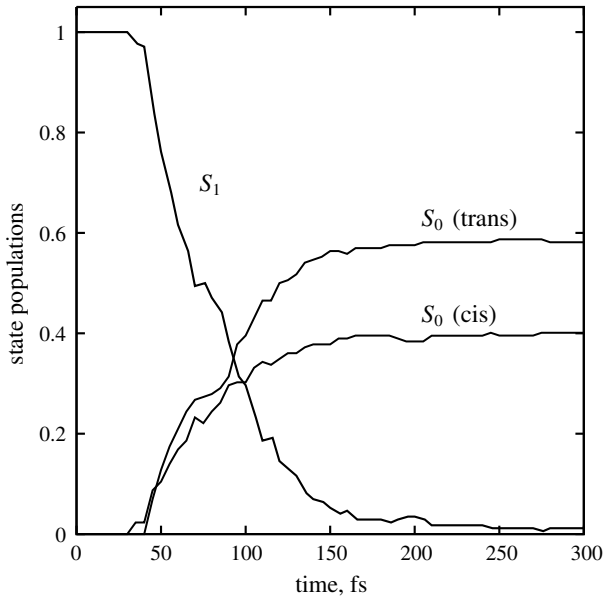

Fig. 5. Time-dependent populations of S_1 and of S_0, the latter split into the *cis* and *trans* isomers.

The photoisomerization mechanism is also quite similar to that of free azobenzene (AB). Fig. 5 shows the population of the excited state as a function of time. The decay is very fast, just as in AB: it starts around $t = 30$ fs, the population drops to 0.5 at 75 fs and almost vanishes after 250 fs. The ultrafast decay is triggered by the torsion of the N=N double bond, which is also the main isomerization mechanism. Fig. 6 shows the CNNC and NNC angles as functions of time, averaged either over the reactive or over the unreactive trajectories. In both cases CNNC rapidly increases just after the excitation, but it goes back to an average of 6° for the unreactive trajectories. For the reactive trajectories, CNNC keeps increasing, while the NNC angles oscillate once towards larger values, because of the shape of the S_1 PES, and then settle at the equilibrium value for the *trans* isomer. However, during the first 1500 fs, the product geometry is rather distorted. Fig. 7 is a typical snapshot, taken at the end of a trajectory. The azobenzene moiety is not planar: in fact, the averaged CNNC angle remains around 160°. This is quite clearly due to the constraints imposed by the H-bond coupling of the cyclopeptides, possibly with some influence of the excess vibrational energy still concentrated in this part of the system.

The geometry keeps changing in the intermediate time range (<1.5 ps), as shown by the time dependence of the averaged distances between pairs of atoms in the $–CH_2–S–CH_2–$ bridges. In Fig. 8 we plot the distance between the carbon atoms directly bound to azobenzene, hereafter denoted as $R_{CC,QM}$; the distance between the carbon atoms

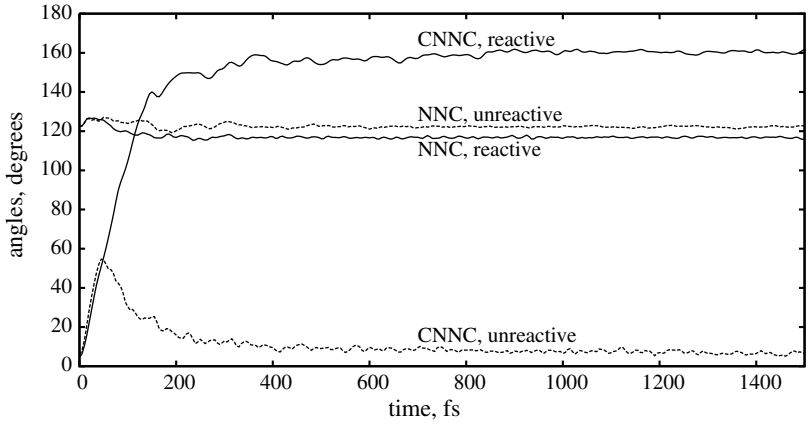

Fig. 6. CNNC and NNC angles as functions of time, averaged over the reactive or over the unreactive trajectories.

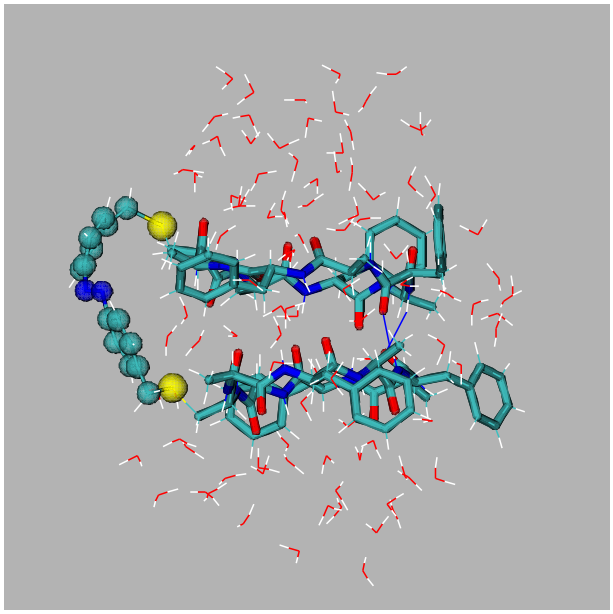

Fig. 7. A typical final configuration ($t = 1.5$ ps) for a trajectory describing the photoisomerization of ABCP.

belonging to the cysteine residues, denoted as $R_{CC,MM}$; and the distance between the sulphur atoms (R_{SS}). For the unreactive trajectories, all three distances go back to the *cis* isomer equilibrium values, after some little initial change. For the reactive trajectories, all three distances do increase over the 1.5 ps time span: we have $\Delta R_{CC,QM} = 3.2$ Å, $\Delta R_{CC,MM} = 2.3$ Å, and $\Delta R_{SS} = 3.4$ Å. The flexibility of the –CH_2–S–CH_2– bridges is exploited, to let the azobenzene moiety isomerize, without spending too much energy in breaking the hydrogen bonds between the cyclopeptides. For this reason, the distances between the atom pairs decrease in going from those rigidly bound to azobenzene ($R_{CC,QM}$), to those already belonging to the peptide system ($R_{CC,MM}$), with the S atoms in an intermediate position.

If we consider the length of the hydrogen bonds, we find an even slower dynamics, not accomplished in 1.5 ps. In Fig. 9 we show the N–O distances of the N···H–O bonds, with the numbering of the aminoacid residues of Fig. 2. The first and second pairs, i.e. the closest to azobenzene, show the largest lengthenings: they start at about 3.2 Å

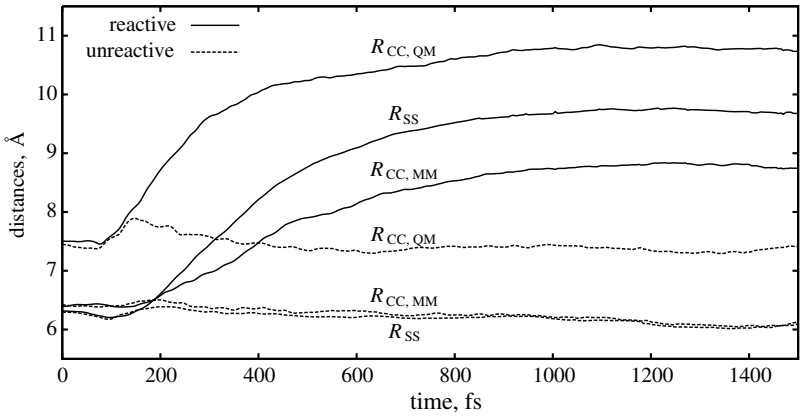

Fig. 8. Distances between pairs of atoms in the –CH_2–S–CH_2– bridges, as functions of time, averaged over the reactive or over the unreactive trajectories. $R_{CC,QM}$ denotes the distance between the carbon atoms directly bound to azobenzene and belonging to the QM subsystem. $R_{CC,MM}$ denotes the distance between the carbon atoms belonging to the cysteine residues and therefore to the MM subsystem. R_{SS} is the distance between the sulphur atoms.

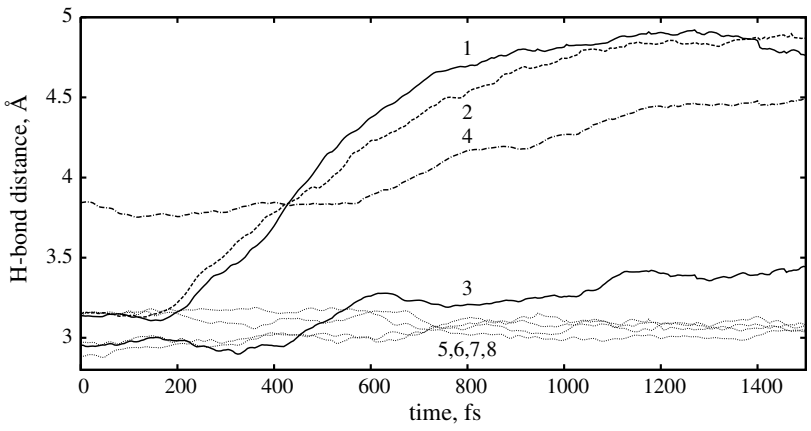

Fig. 9. Distances between N and O atoms involved in the hydrogen bonds, as functions of time, averaged over the reactive trajectories only. The numbering follows that of Fig. 2.

(which is slightly longer than the typical distances for alanine, see for instance Ref. [27]) and end up at about 4.8 Å, which means they are substantially broken. The elongation of these two bonds is simultaneous with that of $R_{CC,MM}$, and follows that of $R_{CC,QM}$. The third H-bond length is initially 2.95 Å (within the typical range) and tends to increase in the first 1.5 ps, up to 3.4 Å. So does the fourth one, which is however much longer (3.8 Å), in the average, since the beginning. In fact, this bond is (partially) broken, at $t = 0$, for a fraction of the trajectories, and its initial length fluctuates more than any of the other ones: its standard deviation is 0.39 Å, while the others are between 0.13 and 0.29 Å. The plots in Fig. 9 suggest that the lengthening of the third and fourth bonds is not completed within the first 1.5 ps. All the other bonds (5th to 8th) are only slightly perturbed by the photoisomerization.

The lengthening of the hydrogen bonds is assisted by the water molecules. In fact, there could be hardly a separation of the two peptide rings, without the formation of new hydrogen bonds of the carbonyl O atoms and of the aminic H atoms with the solvent molecules. In Fig. 10 we show the number of water molecules interacting with the two groups involved in each hydrogen bond, arbitrarily defined as the number of water O atoms found at a distance less than 4.23 Å (8 bohr) from either the carbonyl O or the aminic N. The averages are taken over all the reactive trajectories. We see that the 4th H-bond, which was already broken at the beginning of many trajectories, is the most solvated at all times. Of the three bonds that undergo a noticeable elongation in the first 1.5 ps after excitation, 1 and 3 also increase the number of interacting water molecules, while 2 remains at about the initial number. In the average, the other four bonds show a very modest increase. Overall, these data show that the changes in the solvation structure slowly follow the breaking of the hydrogen bonds: the bond with the largest number of interacting waters remains the 4th one, because it has benefited of a long equilibration time (up to 90 ps of Brownian trajectory before excitation), while 1.5 ps after excitation the rearrangement of the solvent around the other bonds is still moving the first steps.

In addition to, and at the same time of, the structural changes, the system undergoes a redistribution of the vibrational energy. The vertical excitation, and even more the Internal Conversion to S_0, generate a large amount of vibrational energy, initially concentrated in some modes of the azobenzene moiety. Since the potential and kinetic energies are rapidly interconverted (in about 80 fs for a mode with a frequency of 1000 cm^{-1}), we limit ourselves to monitoring the kinetic energy, which can be easily attributed to a specific subset of atoms. It should be noted, however, that the regions of the PES involved in the dynamics are strongly anharmonic, especially before the vibrational energy has been distributed in many modes: therefore, the approximation that the time average of the kinetic energy is half of the total vibrational energy (virial theorem for harmonic potentials) may be a poor one. In Fig. 11 we show the time-dependence of the kinetic energy, averaged over all trajectories, for three subsets of atoms: the QM ones (azobenzene and the attached –CH_2–S– groups, 30 atoms), those belonging to the six aminoacids (three for each peptide ring, 58 atoms) that are closest to azobenzene, and those of the remaining ten aminoacids (160 atoms). The kinetic energy E_K is plotted as a fictitious temperature $T = 2/(3NK_B)$, where N is the number of atoms in the subset and K_B the Boltzmann constant. In this way we eliminate the dependence on the number of atoms and we highlight the differences with respect to the equilibrium thermal energy. We see that the temperature of the QM atoms increases rapidly during the first 180 fs, i.e. about the time required to convert all molecules from S_1 to S_0. We have fitted these data by the phenomenological equation:

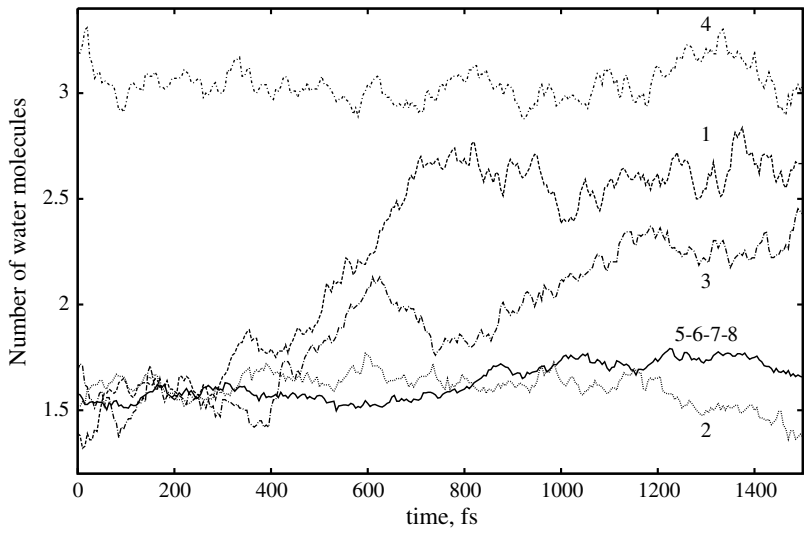

Fig. 10. Number of water molecules found in the proximity of the hydrogen bonded groups, i.e. with the distance of the water O atom from either the aminic N or the carbonyl O smaller than 4.23 Å (8 bohr). Averages over all the reactive trajectories. The numbering of the H-bonds follows that of Fig. 2.

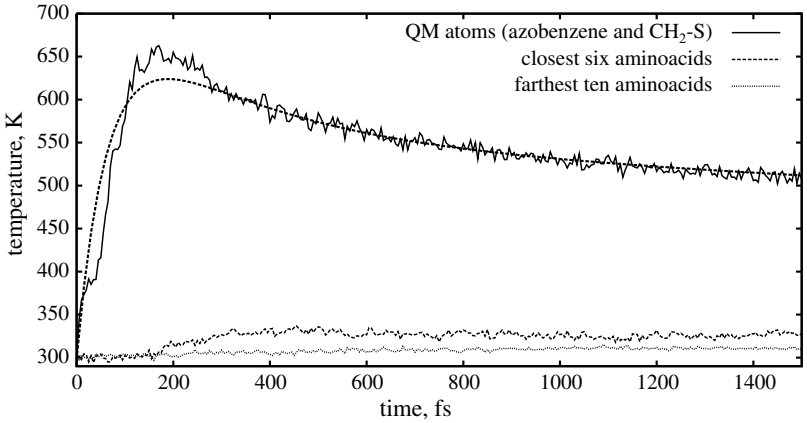

Fig. 11. Total kinetic energy of three subsets of atoms: the QM atoms (azobenzene and the attached –CH_2–S– groups), the six aminoacids (three for each ring) that are closest to azobenzene, and the other 10 aminoacids. The kinetic energy E_K is plotted as a fictitious temperature $T = 2/(3NK_B)$, where N is the number of atoms in a subset. Average over all trajectories. The temperature of the QM atoms is also fitted by the formula of Eq. (10) (dashed line).

$$T(t) = T_\infty + \frac{\Delta E}{3NK_B}[1 - e^{-t/\tau_{rel}}][w_1 e^{-t/\tau_1} + w_2 e^{-t/\tau_2}] \qquad (10)$$

where T_∞ is the equilibrium temperature (298 K) and ΔE is the average excitation energy (79 kcal/mol). τ_{rel} is an overall relaxation time, taking into account the radiationless transition and the conversion of potential energy into kinetic energy. τ_1 and τ_2 are the vibrational energy transfer times, while w_1 and w_2 are weights. The fitting yields $\tau_{rel} = 0.07$ ps, $\tau_1 = 0.3$ ps, $\tau_2 = 8$ ps, $w_1 = 0.42$ and $w_2 = 0.58$. τ_2 is in the range of solvent induced vibrational relaxation times, as can be expected since the azobenzene moiety is only loosely coupled to the rest of the molecule. However, the large weight of the τ_1 component shows that the transfer rate constant can be much larger for a highly excited molecule. The curve concerning the six closest aminoacids shows an increase of the kinetic energy equivalent to ~30 K, after about 0.5 ps, while the ten further ones have only gained ~12 K at the end of the run (1.5 ps).

The structural relaxation and the thermalization, that take place in the ground state on a time scale of several ps, might be monitored by time-resolved differential absorption spectroscopy. This tool has already been applied to detect the ground state recovery time of free azobenzene, yielding times ranging from 10 to 17 ps [28–31]. The $n \rightarrow \pi^*$ band ($S_0 \rightarrow S_1$) of *trans*-azobenzene is very weak, being forbidden by symmetry. It gains intensity by out-of-plane distortions of the chromophore, that may be due to the zero point vibrations, to vibrational excitation occurring at finite temperatures, or to structural constraints [32]. We have simulated the S_0 to S_1, S_2 and S_3 bands of the very distorted and hot azobenzene chromophore, obtained by photoisomerization of *cis*-ABCP (see Ref. [10] for technical details). The results are shown in Fig. 12, for two different time intervals: 200–300 fs (just after isomerization) and 1000–1500 fs (at the end of our simulation runs). The two spectra are similar, with the $n \rightarrow \pi^*$ band stronger than the $\pi \rightarrow \pi^*$ ones. However, at longer times the $S_0 \rightarrow S_2$ absorption makes a distinct shoulder at about 330 nm, while the $n \rightarrow \pi^*$ band decreases in intensity and migrates to shorter wavelengths. These changes are far from being completed at 1.5 ps, and the recovery of the normal absorption spectrum of *trans*-ABCP should be easily detected experimentally.

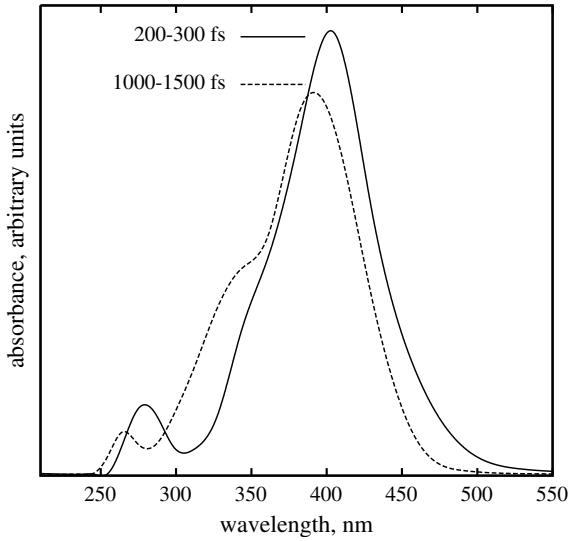

Fig. 12. Simulated absorption spectrum of the *trans*-ABCP resulting from the photoisomerization, for two different time intervals after excitation: 200–300 fs and 1000–1500 fs. Average over all reactive trajectories.

4. Concluding remarks

We have run simulations of the photodynamics with the surface hopping method, on a rather complex system, consisting of azobenzene linked to two cyclopeptides (ABCP), in water solution. The electronic structure and the PES of the system are computed on the fly, during the integration of the nuclear trajectories, by a QM/MM semiempirical method. The results have a paradigmatic value for the problems posed by the azobenzene photoisomerization in supramolecular contexts and by the condensed phase photochemistry in general.

They also show the power of the combination of surface hopping with a direct QM/MM strategy, in tackling large supramolecular systems.

Azobenzene confirms to be able to photoisomerize by the same mechanism, i.e. torsion around the double bond, under different, apparently adverse, conditions [19,25]. In the present case, the *cis*-ABCP isomer is stabilized by the hydrogen bonds formed between the two cyclopeptides. The *cis* → *trans* isomerization following $n \rightarrow \pi^*$ excitation, as well as the excited state decay, is completed after less than 200 fs, but the *trans*-ABCP isomer is very distorted and the whole system undergoes further structural changes for the whole duration of the present simulations, i.e. 1.5 ps. The azobenzene chromophore slowly progresses towards its planar equilibrium structure, while the closest hydrogen bonds are elongated. Some water molecules approach the N–H and C=O groups involved in the hydrogen bonds that are breaking. The complete separation of the two peptide rings, that needs the cooperation of the solvent, would take place in a much longer time. The first steps are accelerated by the photon energy, rapidly converted into vibrational energy, and transferred from the chromophore to the rest of the ABCP molecule within several picoseconds. The simulated absorption spectrum of the distorted *trans*-ABCP is very different from that of the planar azobenzene, and offers a possible way to monitor experimentally the changes that take place after the photoisomerization.

Acknowledgements

This work was supported by grants of the italian M.I.U.R. and of the University of Pisa.

References

[1] M. Asakawa, P.R. Ashton, V. Balzani, C.L. Brown, A. Credi, O.A. Matthews, S.P. Newton, F.M. Raymo, A.N. Shipway, N. Spencer, A. Quick, J.F. Stoddart, A.J.P. White, D.J. Williams, Chem. Eur. J. 5 (1999) 860.
[2] A. Masumi, D.J. Williams, Chem. Eur. J. 5 (1999) 860.
[3] A.N. Shipway, I. Willner, Acc. Chem. Res. 34 (2001) 421.
[4] R. Ballardini, V. Balzani, A. Credi, M.T. Gandolfi, M. Venturi, Acc. Chem. Res. 34 (2001) 445.
[5] C. Dugave, L. Demange, Chem. Rev. 103 (2003) 2475.
[6] C. Cojocariu, P. Rochon, Pure Appl. Chem. 76 (2004) 1479.
[7] K.G. Yager, C.J. Barrett, J. Photochem. Photobiol. A 182 (2006) 250.
[8] L. Gagliardi, G. Orlandi, F. Bernardi, A. Cembran, M. Garavelli, Theor. Chem. Acc. 111 (2004) 363.
[9] A. Cembran, F. Bernardi, M. Garavelli, L. Gagliardi, G. Orlandi, J. Am. Chem. Soc. 126 (2004) 3234.
[10] C. Ciminelli, G. Granucci, M. Persico, Chem. Eur. J. 10 (2004) 2327.
[11] G. Granucci, M. Persico, Theor. Chem. Acc. 117 (2007) 1131.
[12] M.S. Vollmer, T.D. Clark, C. Steinem, M. Reza Ghadiri, Angew. Chem., Int. Ed. 38 (1999) 1598.
[13] C. Steinem, A. Janshoff, M.S. Vollmer, M. Reza Ghadiri, Langmuir 15 (1999) 3956.
[14] J.C. Tully, J. Chem. Phys. 93 (1990) 1061.
[15] J.C. Tully, Faraday Discuss. 110 (1998) 407.
[16] G. Granucci, M. Persico, A. Toniolo, J. Chem. Phys. 114 (2001) 10608.
[17] M. Persico, G. Granucci, S. Inglese, T. Laino, A. Toniolo, J. Mol. Struct. Theochem. 621 (2003) 119.
[18] A. Toniolo, C. Ciminelli, G. Granucci, T. Laino, M. Persico, Theor. Chem. Acc. 93 (2004) 270.
[19] C. Ciminelli, G. Granucci, M. Persico, J. Chem. Phys. 123 (2005) 174317.
[20] W. Qu, H. Tan, G. Chen, R. Liu, Phys. Chem. Chem. Phys. 5 (2003) 2327.
[21] G. Granucci, A. Toniolo, Chem. Phys. Lett. 325 (2000) 79.
[22] D.A. Case, D.A. Pearlman, J.W. Caldwell, T.E. Cheatham III, J. Wang, W.S. Ross, C.L. Simmerling, T.A. Darden, K.M. Merz, R.V. Stanton, A.L. Cheng, J.J. Vincent, M. Crowley, V. Tsui, H. Gohlke, R.J. Radmer, Y. Duan, J. Pitera, I. Massova, G.L. Seibel, U.C. Singh, P.K. Weiner, P.A. Kollman, AMBER 7, University of California, San Francisco, 2002.
[23] W.L. Jorgensen, J. Chandrasekhar, J.D. Madura, R.W. Impey, M.L. Klein, J. Chem. Phys. 78 (1983) 926.
[24] I. Antes, W. Thiel, J. Phys. Chem. A 103 (1999) 9290.
[25] L. Creatini, T. Cusati, G. Granucci, M. Persico, Chem. Phys., in press, doi:10.1016/j.chemphys.2007.09.048.
[26] J.J.P. Stewart, MOPAC 2000 and MOPAC 2002, Fujitsu Limited, Tokyo, Japan.
[27] Y. Wei, D.-K. Lee, A. Ramamoorthy, J. Am. Chem. Soc. 123 (2001) 6118.
[28] I.K. Lednev, T.-Q. Ye, R.E. Hester, J.N. Moore, J. Phys. Chem. 100 (1996) 13338.
[29] I.K. Lednev, T.-Q. Ye, P. Matousek, M. Towrie, P. Foggi, F.V.R. Neuwahl, S. Umapathy, R.E. Hester, J.N. Moore, Chem. Phys. Lett. 290 (1998) 68.
[30] T. Fujino, T. Tahara, J. Phys. Chem. A 104 (2000) 4203.
[31] T. Fujino, S.Yu. Arzhantsev, T. Tahara, Bull. Chem. Soc. Jpn. 75 (2002) 1031.
[32] T. Cusati, G. Granucci, M. Persico, G. Spighi, in preparation.